Gastroenterology 2021;160:1771–1783

Zinc-Dependent Regulation of ZEB1 and YAP1 Coactivation Promotes Epithelial-Mesenchymal Transition Plasticity and Metastasis in Pancreatic Cancer

Mingyang Liu,[1,2,*] **Yuqing Zhang**,[1,2,*] **Jingxuan Yang**,[1,2,*] **Hanxiang Zhan**,[1,2,3,*] Zhijun Zhou,[1,2] Yuanyuan Jiang,[1,2,4] Xiuhui Shi,[1,2] Xiao Fan,[5] Junxia Zhang,[5] Wenyi Luo,[6] Kar-Ming A. Fung,[6] Chao Xu,[7] Michael S. Bronze,[1] Courtney W. Houchen,[1] and Min Li[1,2]

[1]Department of Medicine, the University of Oklahoma Health Sciences Center, Oklahoma City, Oklahoma; [2]Department of Surgery, the University of Oklahoma Health Sciences Center, Oklahoma City, Oklahoma; [3]Department of General Surgery, Qilu Hospital, Shandong University, Jinan, Shandong, China; [4]Department of Pulmonary and Critical Care Medicine, Qilu Hospital, Shandong University, Jinan, Shandong, China; [5]Department of Neurosurgery, the First Affiliated Hospital of Nanjing Medical University, Nanjing, Jiangsu, China; [6]Department of Pathology, the University of Oklahoma Health Sciences Center, Oklahoma City, Oklahoma; [7]Department of Biostatistics and Epidemiology, Hudson College of Public Health, the University of Oklahoma Health Sciences Center, Oklahoma City, Oklahoma

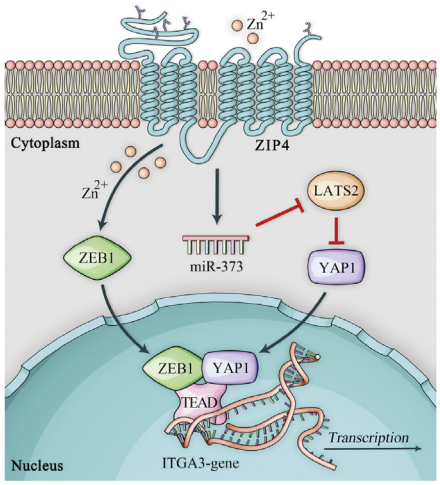

Gastroenterology

BACKGROUND: Pancreatic cancer is characterized by extensive metastasis. Epithelial-mesenchymal transition (EMT) plasticity plays a critical role in tumor progression and metastasis by maintaining the transition between EMT and mesenchymal-epithelial transition states. Our aim is to understand the molecular events regulating metastasis and EMT plasticity in pancreatic cancer. **METHODS:** The interactions between a cancer-promoting zinc transporter ZIP4, a zinc-dependent EMT transcriptional factor ZEB1, a coactivator YAP1, and integrin α3 (ITGA3) were examined in human pancreatic cancer cells, clinical specimens, spontaneous mouse models (KPC and KPCZ) and orthotopic xenografts, and 3-dimensional spheroid and organoid models. Correlations between ZIP4, miR-373, and its downstream targets were assessed by RNA in situ hybridization and immunohistochemical staining. The transcriptional regulation of ZEB1, YAP1, and ITGA3 by ZIP4 was determined by chromatin immunoprecipitation, co-immunoprecipitation, and luciferase reporter assays. **RESULTS:** The Hippo pathway effector YAP1 is a potent transcriptional coactivator and forms a complex with ZEB1 to activate ITGA3 transcription through the YAP1/transcriptional enhanced associate domain (TEAD) binding sites in human pancreatic cancer cells and KPC-derived mouse cells. ZIP4 upregulated YAP1 expression via activation of miR-373 and inhibition of the YAP1 repressor large tumor suppressor 2 kinase (LATS2). Furthermore, upregulation of ZIP4 promoted EMT plasticity, cell adhesion, spheroid formation, and organogenesis both in human pancreatic cancer cells, 3-dimensional spheroid model, xenograft model, and spontaneous mouse models (KPC and KPCZ) through ZEB1/YAP1-ITGA3 signaling axis. **CONCLUSION:** We demonstrated that ZIP4 activates ZEB1 and YAP1 through distinct mechanisms. The ZIP4-miR-373-LATS2-ZEB1/YAP1-ITGA3 signaling axis has a significant impact on pancreatic cancer metastasis and EMT plasticity.

Keywords: Transcription Coactivation; Zinc Homeostasis; Post-transcriptional Regulation.

Pancreatic cancer is the third leading cause of cancer-related death in the United States, and has an overall survival rate of only 9%.[1] More than 60% of patients with pancreatic cancer had distant metastasis within the first 24 months after surgery.[2] Pancreatic cancer metastasis requires cell detachment, migration, invasion, and adhesion. Epithelial-mesenchymal transition (EMT) is an essential process for tumor metastasis, and is activated by pathogenic stimuli and promotes the whole course of early- to late-stage metastasis. EMT plasticity is a dynamic program that transits between EMT and mesenchymal-epithelial transition (MET) phenotypes to facilitate tumor metastasis.[3] At the same time, adhesion is required for endothelial cells to form stronger bonds, attach at the new location, and proliferate to produce the secondary tumor.[4] Integrins are transmembrane receptors that are upregulated on the cell surface and correlate with increased metastatic capacity of tumor cells.[5] Control of EMT and cell adhesion are essential for regulation of pancreatic cancer metastasis.

EMT is mediated by a set of EMT-activating transcription factors (EMT-TFs) including Snail, Slug, Twist1, ZEB1, and ZEB2. Most EMT-TFs except Twist1 are zinc finger proteins.[6] These factors are overexpressed in many cancers, including bladder, breast, colon, and pancreatic cancer. EMT-TFs act as transcription repressors by reducing epithelial markers during embryonic development and tumor progression.[7–9] ZEB1 is the most important EMT-TF in pancreatic cancer, which promotes stemness, invasion, and metastasis in pancreatic cancer, as shown in the KPC and KPC ZEB1 knockout mouse models.[10] ZEB1 normally acts as a transcription repressor to inhibit downstream target transcription including E-cadherin and miR-200 family members[11] through binding to E-box motif at their promoter regions. However, ZEB1 also can switch from a transcription repressor to transcription activator on interacting with coactivators such as Lef1, YAP1, P300, and Smad, which belong to other regulatory and cancer-promoting pathways such as Hippo and Wnt pathway.[12–14] Hippo pathway controls cell shape, organ size, tissue regeneration, tumorigenesis, EMT, and cell adhesion. YAP1 is a major downstream effector of Hippo pathway and activation of YAP1 leads to lung, colon, and pancreatic cancer carcinogenesis and tumor progress.[15–17] However, how these 2 pathways interact and what functional impact this interaction has remains unknown in pancreatic cancer. The large tumor suppressor 2 kinase (LATS2) is one of the Hippo pathway kinases that directly phosphorylates YAP1 and inhibits YAP1 activity by protein degradation, thereby inhibiting transcription of downstream targets of YAP1. Moreover, inhibition of LATS2 increases the YAP1/transcriptional enhanced associate domain (TEAD) interaction, leading to YAP1/TEAD transcriptional activation.[18] YAP1/TEAD complex activates their oncogenic downstream genes such as CTGF and c-Myc, leading to gastric cancer carcinogenesis.[19] Several studies show that microRNAs (miRNAs), including let-7, miR-10b, and miR-183, are involved in the regulation of the Hippo pathway.[20,21] LATS2 is a direct target of miR-373 in pancreatic cancer and inhibition of LATS2 promoted tumor growth.[22] The specific mechanism of miRNA-LATS2 regulation in pancreatic cancer also remains to be elucidated.

In the current study, we identified a novel function of a cancer-promoting zinc transporter ZIP4 in EMT plasticity and cell–extracellular matrix (ECM) adhesion induced by ZEB1-integrin in both 2-dimensional (2D) and 3-dimensional (3D) culture conditions. We found that ZIP4 promoted EMT plasticity and pancreatic cancer cell-laminin adhesion and enhanced spheroid and organoid formation through activating integrins. We also found that knock down of ZEB1 significantly inhibited organogenesis and apical to

WHAT YOU NEED TO KNOW

BACKGROUND AND CONTEXT

Pancreatic cancer is characterized by extensive metastasis. EMT plasticity plays a critical role in tumor progression and metastasis by maintaining the transition between EMT and MET states. Our aim is to understand the molecular events regulating metastasis and EMT plasticity in pancreatic cancer.

NEW FINDINGS

The Hippo pathway effector YAP1 is a potent transcriptional co-activator and forms a complex with ZEB1 to activate ITGA3 transcription through the YAP1/TEAD binding sites in human pancreatic cancer cells and KPC derived mouse cells. ZIP4 upregulated YAP1 expression via activation of miR-373 and inhibition of the YAP1 repressor LATS2. Furthermore, upregulation of ZIP4 promoted EMT plasticity, cell adhesion, spheroid formation and organogenesis both in human pancreatic cancer cells, 3D spheroid model, xenograft model, and spontaneous mouse models (KPC and KPCZ) through ZEB1/YAP1-ITGA3 signaling axis.

LIMITATIONS

The role of other EMT transcription factors were not included in this study.

IMPACT

We demonstrated that ZIP4 activates ZEB1 and YAP1 through distinct mechanisms. The ZIP4-miR-373-LATS2-ZEB1/YAP1-ITGA3 signaling axis has a significant impact on pancreatic cancer metastasis and EMT plasticity.

* Authors provided equal contributions.

Abbreviations used in this paper: ChIP, chromatin immunoprecipitation; ECM, extracellular matrix; EMT, epithelial-mesenchymal transition; EMT-TF, EMT-activating transcription factor; ITGA3, integrin α3; LATS2, large tumor suppressor 2 kinase; MET, mesenchymal-epithelial transition; miRNA, microRNA; mYAP1, mouse YAP1; PBS, phosphate-buffered saline; siRNA, small interfering RNA; OUHSC, University of Oklahoma Health Sciences Center; TCGA, The Cancer Genome Atlas; TEAD, transcriptional enhanced associate domain; WT, wild type; 2D, 2-dimensional; 3D, 3-dimensional.

Most current article

0016-5085/$36.00
https://doi.org/10.1053/j.gastro.2020.12.077

basal polarity in a 3D organoid model derived from KPC ZEB1 knockout cell lines. We further elucidated the mechanism showing that ZEB1 activated ITGA3 through binding to the YAP1/TEAD binding sites at ITGA3 promoter region and ZIP4 upregulated YAP1 expression via miR-373-LATS2 axis. These findings show a novel molecular link between ZIP4 and EMT, cell-ECM adhesion, and pancreatic cancer organogenesis, this essential link may serve as the foundation for the development of new therapeutic strategies for this devastating disease.

Materials and Methods

Cell Lines, Small Interfering RNAs, and Plasmids

Human pancreatic cancer cell lines AsPC-1 and MIA PaCa-2 were purchased from American Type Culture Collection (ATCC, Rockville, MD), and were cultured in RPMI 1640 medium or Dulbecco's modified Eagle's medium with 10% fetal bovine serum. KPC and KPC-ZEB1 knockout (KPCZ) cells were kindly provided by Dr Thomas Brabletz, University of Erlangen-Nürnberg, Germany. All cell lines were authenticated and verified to be mycoplasma free using MycoAlert kit (Lonza, Basel, Switzerland). ITGA3, YAP1, and LATS2 small interfering RNAs (siRNAs) were purchased from Santa Cruz Biotechnology (Dallas, TX). Mimic and inhibitor of miR-373–3p were purchased from Ambion (Austin, TX). hZEB1 and mouse YAP1 (mYAP1) ORF plasmids were purchased from Genecopoeia (Rockville, MD), while the hYAP1 ORF plasmid was obtained from Addgene (Cambridge, MA; catalog number 42555).

Human Tissue Samples

Human pancreatic cancer tissue specimens were obtained from the University of Oklahoma Health Sciences Center (OUHSC). This study was approved by the institutional review board at OUHSC. Banked de-identified tissues were used. Written consent from all subjects was obtained.

Stable Cell Line Construction

Stable pancreatic cancer cell lines MIA-V, MIA-ZIP4, AsPC-shV, AsPC-shZIP4, MIA-ZIP4-Pre-C, MIA-ZIP4-Pre-miR-373, AsPC-shZIP4-Anti-C, and AsPC-shZIP4-Anti-miR-373 cells were generated as previously described.[22–24] The MIA-ZEB1/YAP1 overexpression stable cell line was selected using the lentivirus vector from Genecopoeia and Addgene following the manufacturer's instructions. Briefly, human ZEB1 ORF was cloned into the pEZ-Lv207 vector and human YAP1 ORF was cloned into pLX304 vector. Viral supernatants were collected and transduced to the target cells. Stable cell lines expressing ZEB1 were selected using 200 μg/mL Hygromycin B and stable cell lines expressing YAP1 were selected with 10 μg/mL Blasticidin.

Spheroid Formation Assay

Cells were resuspended in culture medium containing 0.24% methylcellulose (Sigma, M0512). And then were seeded onto inside of the lid of 10 cm^2 dishes with 20 μL per drop. Lids were inverted over dishes containing 10 mL phosphate-buffered saline (PBS). Spheroids were cultured at 37 °C and then imaged using a light microscope at 2, 4, and 24 hours post seeding. Ten spheroids were included and analyzed in each group.

Three-Dimensional Organoid Culture

Matrigel-embedded organoid: The chamber slides were precoated with growth factor reduced Matrigel (Corning, Corning, NY) at 37°C for 2 hours. After rinsing with PBS, the single cell suspension mixed with 10 ng/mL epidermal growth factor, 10 μg/mL insulin, and 2% Matrigel was seeded onto the chamber slide at 8×10^3 cells per well. The slides were incubated at 37 °C overnight. The cells were cultured with fresh medium containing 10 ng/mL epidermal growth factor and 10 μg/mL insulin and replenished every 3 days. The cells formed clusters by day 6 to day 8.

Matrigel-suspended organoid: The organoids were also generated by seeding the cell suspension with 50% Matrigel onto the 24-well plate with 5×10^5 cells/mL; the 24-well plate was incubated at 37 °C overnight. The cells were refed as previously and cells formed clusters at multiple layers by day 6 to day 8.

Chromatin Immunoprecipitation Assay

The chromatin immunoprecipitation (ChIP) assay was performed in AsPC-1 cells by using the anti-ZEB1, YAP1, and TEAD antibody (Cell Signaling Technology, Danvers, MA) with the MAGnif Chromatin Immunoprecipitation System (Life Technologies, Carlsbad, CA) following the standard protocol. After the antibody pulling down, the target DNA fragment was amplified and determined by polymerase chain reaction. Primers were designed within YAP1/TEAD binding sites at the ITGA3 promoter region.

Promoter Activity Assay

ITGA3 promoter sequence was generated from USCS genomic browser. The 930-base pair promoter regions of ITGA3 were cloned into pGL4.10-basic reporter vector as previously described.[25] Promoter sequence of ITGA3 was uploaded to the JASPAR database. The threshold was set to 70%. YAP1/TEAD binding sites were predicted through the JASPAR database.[26] The mutant ITGA3 promoter vector was constructed with YAP1/TEAD binding sites mutated at ITGA3 promoter region. The wild-type (WT) and mutant ITGA3 promoter vector were co-transfected with control plasmid pRL-TK into AsPC-1 and MIA PaCa-2 cells. The promoter activity was determined by a Dual-Luciferase Reporter Assay (Promega, Madison, WI).

Co-Immunoprecipitation

MIA-ZEB1/YAP1 cells were lysed, and anti-ZEB1, YAP1, and TEAD (Cell Signaling Technology) antibodies (1–10 μg) were diluted in 200 μL of Ab binding and washing buffer and incubated with rotation for 10 minutes at room temperature and the magnetic bead-Ab complex was washed with washing buffer. The magnetic bead-Ab-Ag complex was incubated with rotation for 20 minutes at room temperature to allow the antigen to bind to the magnetic bead-Ab complex; 20 μL elution buffer and 10 μL of pre-mixed NuPAGE LDS sample buffer and NuPAGE sample reducing agent were added to the complex and heated for 10 minutes at 70°C. The supernatant containing

eluted Ab and Ag was transferred to a clean tube and loaded onto the sodium dodecyl sulfate gel for Western Blotting.

RNA Basescope In Situ Staining

Pancreatic cancer tissues were freshly sectioned at 4 to 5 μm. miR-373 BaseScope LS Reagents (Advanced Cell Diagnostics Inc., Newark, CA) were loaded onto the Staining System. Tissue sections were deparaffinized on the instrument, followed by epitope retrieval, miR-373 probe hybridization, signal amplification, colorimetric detection, and counterstaining. Dihydrodipicolinate reductase and peptidyl-prolyl cis-trans isomerase B were used as the negative and positive control probes, respectively.

Pancreatic Cancer Xenograft Mouse Model

MIA-ZIP4-Anti-C, MIA-ZIP4-Anti-miR-373, AsPC-shZIP4-Pre-C, AsPC-shZIP4-Pre-miR-373 MIA-ZIP4 shV, MIA-ZIP4 sh-ITGA3 stable cell lines were used to generate the orthotopic xenograft tumor model as previously described.[22,25] Briefly stable pancreatic cancer cells were harvested and resuspended in Dulbecco's modified Eagle's medium or RPMI medium; 3×10^6 cells in 50 μL culture medium were injected into the pancreases of 5- to 6-week-old nude mice. The peritoneum and skin were closed with 4.0 surgical sutures. All mice were cared for in accordance with the Office for Protection from Research Risks and Animal Welfare Act Guidelines under an animal protocol approved by the Animal Welfare Committee at OUHSC. After 5 to 6 weeks, all surviving mice were euthanized by CO_2 asphyxiation and tumor tissues were collected and fixed in formalin.

Statistical Analysis

Quantitative results are shown as means ± standard deviation (SD). Overall differences among groups were assessed by analysis of variance and post hoc Dunnett's multiple comparison tests were used to compare data from control and each treated group. Two-group comparisons were analyzed by Student t tests. A P value of $< .05$ was considered statistically significant. All tests were 2-sided. Further details of the Materials and Methods are found in the Supplementary Materials and Methods.

Results

YAP1 Is a Potent Coactivator of ZEB1 to Enhance ITGA3 Transcription in Pancreatic Cancer Cells

Previously we have shown that a zinc-dependent activation of ZEB1 promotes pancreatic cancer growth and chemoresistance.[25] We thus sought to determine how ZEB1 activates the integrin pathway and promotes pancreatic cancer progression, metastasis, and EMT plasticity. ZEB1 switches from a transcription repressor to a transcription activator when coactivators are recruited to the same locus in the promoter region, therefore we examined the potential coactivators of ZEB1 in human pancreatic cancer cells. YAP1, Lef1, CAF, and P300 have been reported to serve as transcriptional coactivators in several cancers,[12–14] and were upregulated in pancreatic cancer compared with normal pancreas as shown in The Cancer Genome Atlas (TCGA) and GTEx database (Supplementary Figure 1*A*). We knocked down all 4 coactivators; only YAP1 knockdown significantly inhibited the promoter activity and reduced the messenger RNA level of ITGA3 in MIA PaCa-2 and AsPC-1 cells (Figure 1*A* and *B*, Supplementary Figure 1*B* and *C*). The TCGA database also showed that YAP1 positively correlates with ZIP4, ZEB1, and ITGA3 (Supplementary Figure 1*D*–*F*). ZIP4 also upregulated YAP1 both in human pancreatic cancer cell lines and xenograft tumor tissues (Supplementary Figure 1*G*–*J*). We thus concluded that YAP1 is the potential coactivator of ZEB1, and can be upregulated by ZIP4 in pancreatic cancer. We then performed gene set enrichment analysis of ZEB1 and YAP1 expression profiles in the TCGA database and found that gene sets of YAP1 are significantly enriched in ZEB1 highly expressed group (Supplementary Figure 1*K*). We analyzed the promoter region of ITGA3 and found YAP1 was enriched and shared the transcriptional peak call with ZEB1 at the same locus of ITGA3 promoter according to the ChIP sequencing data (Supplementary Figure 1*L*). These data show that ZEB1-mediated upregulation of ITGA3 is dependent on the YAP1 status in pancreatic cancer.

ZEB1 Activates ITGA3 Transcription Through YAP1/TEAD Binding Sites

To further investigate whether YAP1 directly activates ITGA3 in pancreatic cancer, we performed ChIP–polymerase chain reaction assay; ZEB1 and YAP1 bound to the same region of the ITGA3 promoter (Figure 1*C*). Based on the luciferase reporter assay results, we found that knockdown of YAP1 inhibited the promoter activity of ITGA3 even when ZIP4 was overexpressed (Figure 1*D*), indicating that the transcriptional activation of ITGA3 may require the presence of YAP1. We also found blocking of YAP1 through siRNA decreased ITGA3 expression and overexpression of YAP1 rescued the inhibition of ZIP4 on ITGA3 expression (Figure 1*E*, Supplementary Figure 2*A* and *B*). We also overexpressed mYAP1 in WT KPC and ZEB1 knockout KPCZ mouse cell lines; overexpression of mYAP1 increased ITGA3 level in KPC cells but not in KPCZ cells (Figure 1*F*, Supplementary Figure 2*C* and *D*), suggesting that the YAP1 activated ITGA3 requires ZEB1. Although YAP1 is a transcriptional coactivator, it does not have DNA-binding domains but regulates gene expression through TEAD1–4.[27] The JASPAR database[26] predicts there are 10 TEAD1–4 binding sites in the ITGA3 promoter. We generated double mutations at the binding sites that are with the highest scores at the JASPAR database (Supplementary Figure 2*E*), and found that sequential mutation of the TEAD binding sites inhibited co-stimulation of the ITGA3 promoter by ZEB1 and YAP1 (Figure 1*G* and *H*, Supplementary Figure 2*F* and *G*). This indicates that the YAP1/TEAD binding sites are essential for ZEB1 stimulation of ITGA3 transcription. We further investigated whether ZEB1 and YAP1 directly interact to coactivate ITGA3. We performed co-immunoprecipitation assays and as expected YAP1 and TEAD directly interacted with each other; ZEB1 and TEAD also interacted in the pancreatic cancer cells (Figure 1*I*). It is

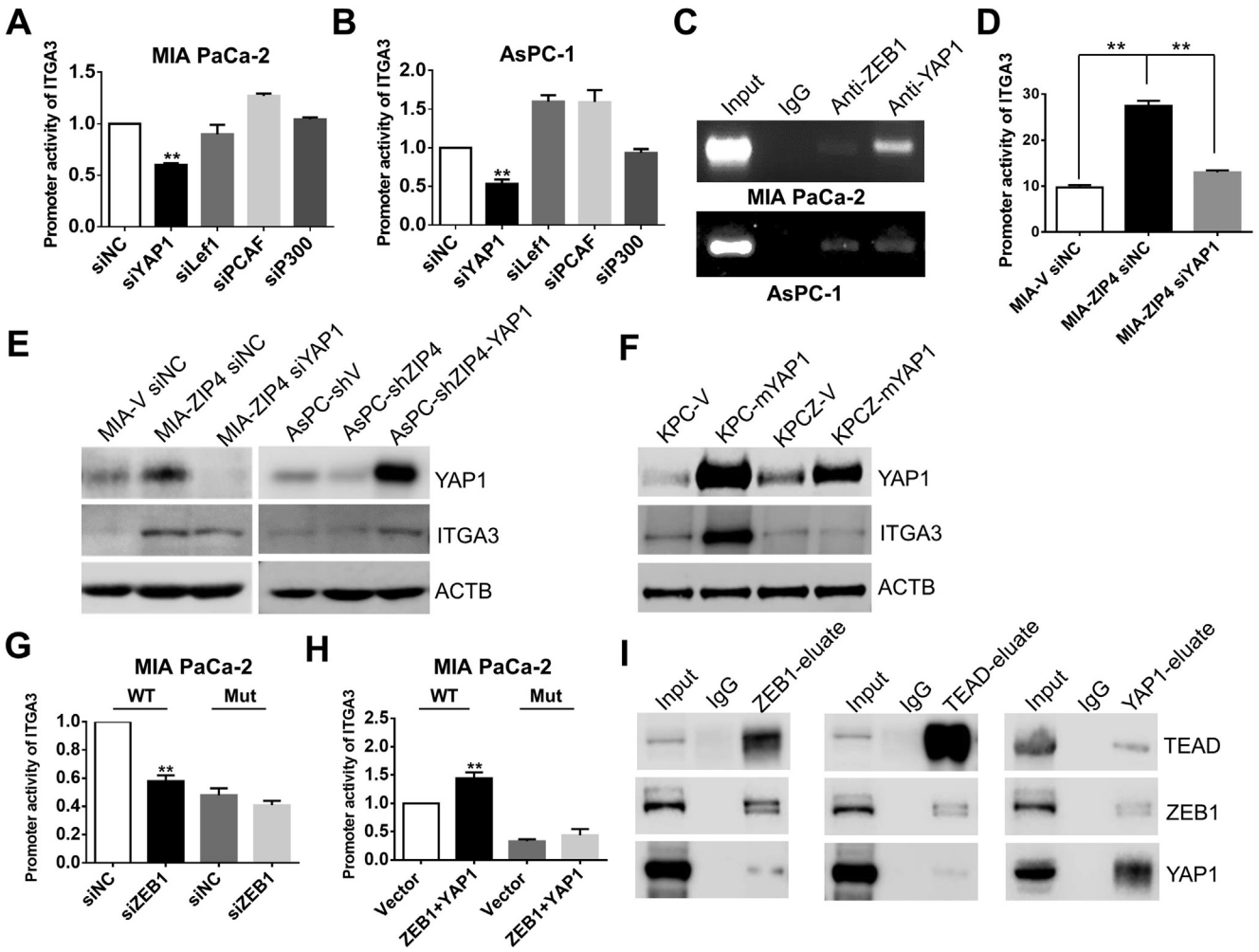

Figure 1. ZEB1 activates ITGA3 transcription through YAP1's binding sites at ITGA3 promoter. (*A*) Promoter activity of ITGA3 in MIA PaCa-2 siYAP1, siLef1, siCAF, and siP300 cells. (*B*) Promoter activity of ITGA3 in AsPC-1 siYAP1, siLef1, siCAF, and siP300 cells. (*C*) ChIP–polymerase chain reaction. ChIP binding assay with anti-ZEB1 and anti-YAP1 in MIA PaCa-2 and AsPC-1 cells confirms the binding of ZEB1and YAP1 to the ITGA3 promoter region. (*D*) Promoter activity of ITGA3 in MIA-V siNC, MIA-ZIP4 siNC, and MIA-ZIP4 siYAP1 cells. $^{**}P < .01$. (*E*) Expression of YAP1 and ITGA3 in PC cells with YAP1 high or low. (*F*) Expression of YAP1 and ITGA3 in KPC and KPCZ cells with mYAP1 overexpressed. Empty vector and mYAP1 ORF vector were transiently transfected into KPC and KPCZ cells. (*G*) Promoter activity of ITGA3 in MIA PaCa-2 cell transfected with WT or mutation vector (YAP1 binding sites). siRNA of ZEB1 was co-transfected with ITGA3 promoter vector. $^{**}P < .01$. (*H*) Promoter activity of ITGA3 in MIA PaCa-2 cell transfected with WT or mutation vector (YAP1 binding sites). ORF vectors of ZEB1/YAP1 was co-transfected with ITGA3 promoter vector. $^{**}P < .01$. (*I*) Co-immunoprecipitation in MIA PaCa-2-ZEB1/YAP1 cells.

established that the protein structure of YAP1 contains several domains including a WW domain, a TEAD transcription factor–interacting domain, a transcription activation domain, and a PDZ domain-binding motif.[28] We sought to investigate which domain contributes to ITGA3 transcriptional activation. We transfected MIA PaCa-2 cells with the empty vector, WT YAP1 vector, YAP1-TEAD TID mutated vector, YAP1-PDZ deletion vector, YAP1-WW mutated vector, and YAP1-phosphorylation mutated vector respectively (Supplementary Figure 3*A*); only mutation of TID domain decreased ITGA3 expression but did not affect YAP1 level (Supplementary Figure 3*B*) compared with the WT YAP1 vector. Mutation of the TID domain significantly reduced ITGA3 transcription (Supplementary Figure 3*C*), whereas mutation of the other 3 domains had no significant impact on the transcription of ITGA3 in pancreatic cancer cells (Supplementary Figure 3*D*–*F*). In addition, the YAP1 inhibitor verteporfin, which is known to reduce YAP1/TEAD activity and deactivate YAP1 targets,[29] was used to treat MIA-ZIP4 cells and inhibited expression of ITGA3 (Supplementary Figure 3*G*). In total, these data demonstrated that the transcription coactivator YAP1 is required for ITGA3 transcriptional activation and that ZEB1 activates ITGA3 through YAP1/TEAD binding sites.

ZIP4 Upregulates YAP1 Through miR-373-LATS2 in Pancreatic Cancer Cells

The preceding results showed that ZEB1 and YAP1 cooperatively stimulate ITGA3 transcription. ZEB1 can be

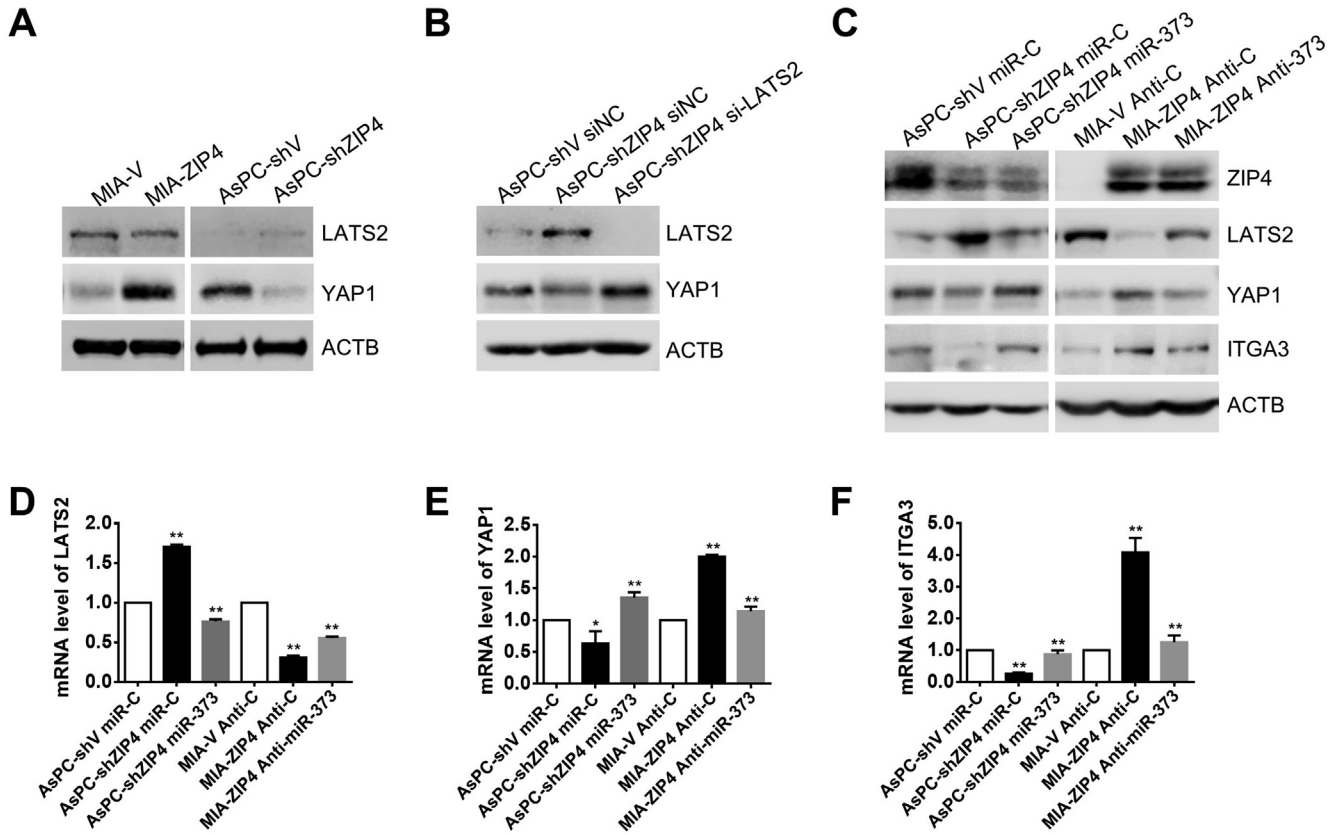

Figure 2. ZIP4 upregulates YAP1 through miR-373-LATS2 in pancreatic cancer cells. (*A*) Expression of YAP1 and LATS2 in MIA-V, MIA-ZIP4, AsPC-shV, and AsPC-shZIP4 cells. (*B*) Expression of YAP1 and LATS2 in AsPC-shZIP4 cells with LATS2 knockdown. (*C*) Protein levels of LATS2, YAP1, and ITGA3 in AsPC-shV miR-C, AsPC-shZIP4 miR-C, AsPC-shZIP4 miR-373, MIA-V Anti-C, MIA-ZIP4 Anti-C, and MIA-ZIP4 Anti-miR-373 cells. (*D–F*) Messenger RNA levels of LATS2, YAP1, and ITGA3 in AsPC-shV miR-C, AsPC-shZIP4 miR-C, AsPC-shZIP4 miR-373, MIA-V Anti-C, MIA-ZIP4 Anti-C, and MIA-ZIP4 Anti-miR-373 cells. $^{*}P < .05$, $^{**}P < .01$.

activated by ZIP4 in a zinc-dependent manner[25]; however, whether YAP1 is also regulated by ZIP4 in pancreatic cancer is unknown. In this study, we found that ZIP4 significantly upregulated YAP1 expression in pancreatic cancer cells, whereas knock down of ZIP4 decreased YAP1 (Figure 2*A*). Having shown an impact of ZIP4 on YAP1 levels, we sought to elucidate how ZIP4 upregulates YAP1 in pancreatic cancer. YAP1 is known to be inhibited by large tumor suppressor 1/2 (LATS2) via its effects on YAP1 phosphorylation and cytoplasmic localization, ubiquitination, and degradation.[30] We found that YAP1 inversely correlated with LATS2 in human pancreatic cancer cells (Figure 2*A*, Supplementary Figure 4*A*), and that knock down of ZIP4 inhibited YAP1 expression but further blocking of LATS2 with siRNA rescued YAP1 level (Figure 2*B*, Supplementary Figure 4*B*). Knockdown of ZIP4 also decreased YAP1 nuclear translocation (Supplementary Figure 4*C*). We have previously shown that ZIP4 downregulated LATS2 via activating a CREB-miR-373 signaling axis,[22] we sought to determine whether ZIP4 upregulates YAP1 through an miR-373-LATS2 signaling pathway. Overexpression of miR-373 inhibited LATS2 but increased YAP1 and ITGA3 expression, whereas blocking miR-373 increased LATS2 level but inhibited YAP1 and ITGA3 expression (Figure 2*C–F*, Supplementary Figure 4*D–H*). To assess the impact of miR-373 on YAP1 and ITGA3 in vivo, we used orthotopic xenograft tumor models; either AsPC-shZIP4-pre-miR-373 or MIA-ZIP4-Anti-373 stable cell lines were injected into the pancreas of the nude mouse (Supplementary Figure 4*I*). To validate this apparent correlation between ZIP4 and miR-373, we assessed miR-373 and ZIP4 levels using RNA Basescope in situ and immunohistochemical staining in 35 human pancreatic cancer tissues. miR-373 colocalized with ZIP4 in the tumor tissue, and when expression of ZIP4 was high, miR-373 levels were also high (Figure 3*A*). We determined protein levels of LATS2, YAP1, and ITGA3 in the xenograft tumor tissues from both models. In the miR-373 overexpressed tumor model, LATS2 levels were lower and YAP1 and ITGA3 expression was higher, whereas in the miR-373–inhibited animals, LATS2 levels increased but YAP1 and ITGA3 levels decreased (Figure 3*B*). We also assessed correlations between LATS2, YAP1, and ITGA3 in the human pancreatic cancer tissues and adjacent normal pancreatic tissues; we found correlations in levels of these proteins, when YAP1 and ITGA3 were high, the expression of LATS2 was low (Figure 3*C* and Supplementary Figure 5*A* and *B*). In addition, we found that YAP1 and ZEB1 colocalized in these

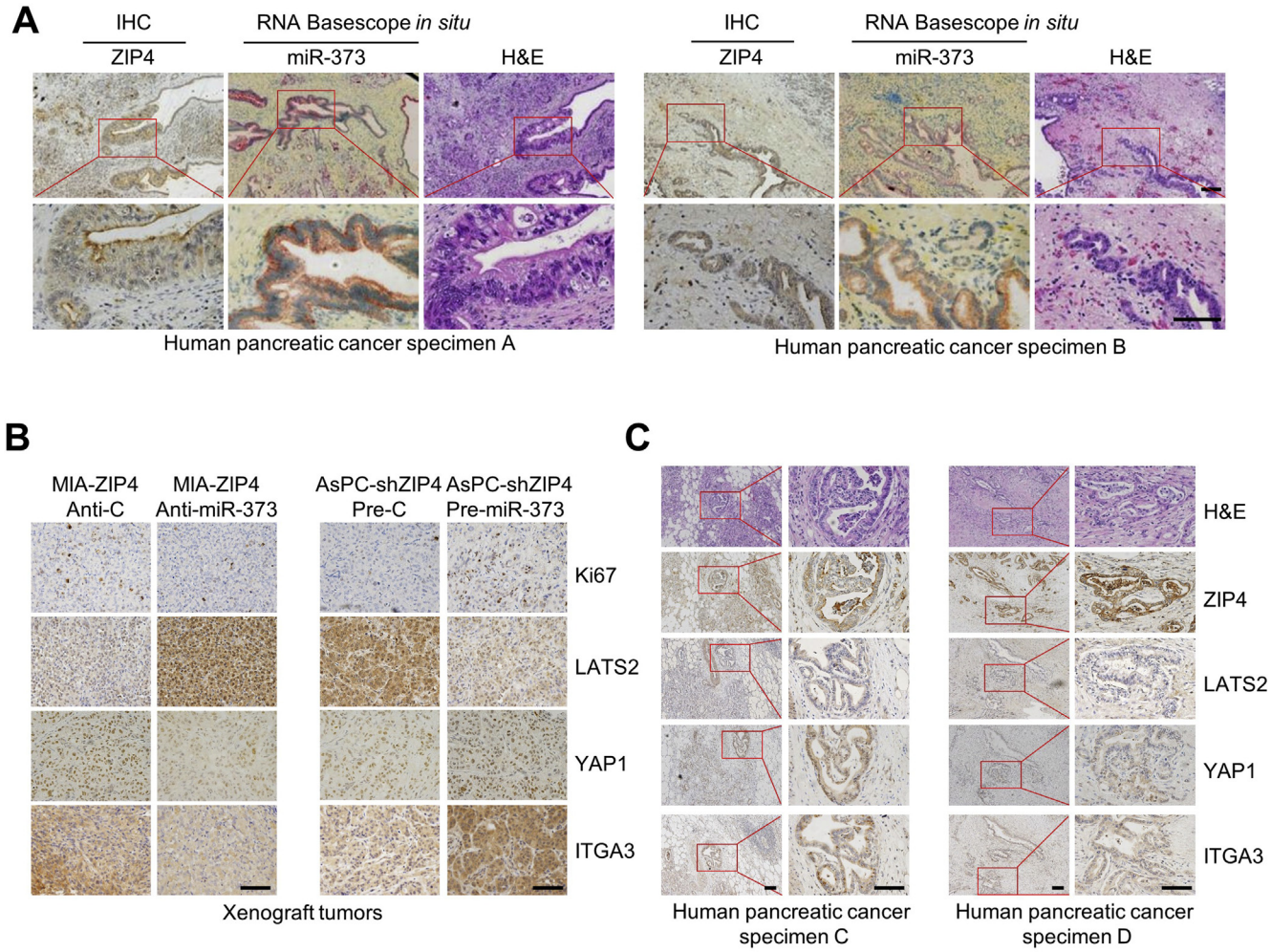

Figure 3. miR-373 upregulates ITGA3 through LATS2-YAP1 in pancreatic cancer in vivo. (*A*) RNA Basescope in situ staining with miR-373 and ZIP4 immunohistochemical staining in human pancreatic cancer tissues indicated the colocalization of miR-373 and ZIP4. Scale bar = 50 μm. (*B*) Immunohistochemical staining of Ki67, LATS2, YAP1, and ITGA3 in the xenograft tumor tissues. Scale bar = 50 μm. (*C*) immunohistochemical staining of ZIP4, LATS2, YAP1, and ITGA3 in human pancreatic cancer tissues. Scale bar = 50 μm.

human pancreatic cancer tissues (Figure 3*C*, Supplementary Figure 5*B*). These findings indicate that ZIP4 upregulates YAP1 by activating an miR-373-LATS2 signaling pathway in pancreatic cancer.

ZIP4 Promotes Cell Adhesion, Spheroid Formation, and Organogenesis Through Its Downstream Target ITGA3

Organogenesis is important for tumor initiation and cell adhesion and it supports metastatic colonization in the late stage of metastasis. To further understand the underlying mechanism of tumor progression and metastasis, we interrogated the effect of ZIP4 on organogenesis and cell adhesion. We have shown that ZIP4 is vital for pancreatic cancer cell proliferation, metastasis, and chemoresistance.[22–25,31,32] In addition, our GO analysis of the TCGA database showed that ZIP4 also contributes to pancreatic cancer cell motility and cell-matrix adhesion. To determine the function of ZIP4 in modulating cell adhesion, we first performed adhesion assays and found that ZIP4 increased laminin-induced cell adhesion in pancreatic cancer cell lines (Figure 4*A*); however, the lack of structural architecture in a 2D model makes it difficult to assess the specific role of ZIP4 in cell adhesion. The recent development of 3D tumor spheroid and organoid cultures allows for this type of study because they better simulate and recapitulate the biology of tumors than 2D cell monolayers.[33] We analyzed the morphology of spheroids following 2, 4, and 24 hours of spheroid culture. Spheroids aggregated more rapidly when ZIP4 was overexpressed, but blocking of ZIP4 inhibited the spheroid formation (Figure 4*B*). We additionally investigated the effect of ZIP4 on organogenesis using 3D organoid culture following 8 days of organoid culture. ZIP4 overexpressing cells showed more organoid clusters of larger size, and with increased density and a more integrated structure (Figure 4*C–E*); however, when ZIP4 was knocked down in AsPC-1 cells, the organoid size was decreased in both Matrigel-embedded

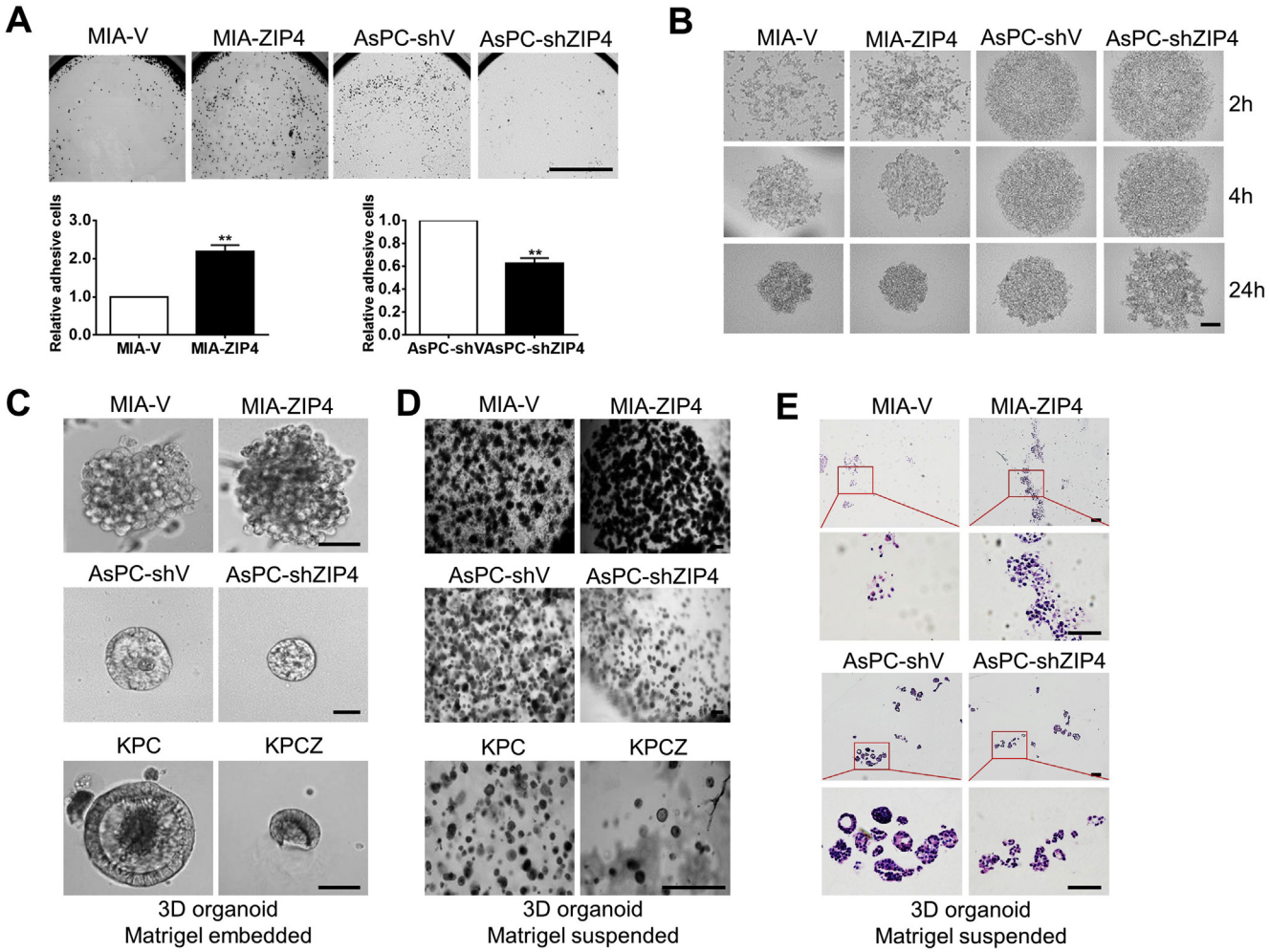

Figure 4. ZIP4 enhances cell-ECM adhesion and spheroid/organoid formation. (*A*) Adhesion assay: 96-well plates were precoated with 500 μg/mL Laminin for 2 hours. MIA-V, MIA-ZIP4, AsPC-shV, and AsPC-shZIP4 cells were seeded in a 96-well plate for 30 minutes at 37°C, then cells were gently washed with phosphate-buffered saline 2 times. Absorbance was recorded at 490 nm to determine the percentage of cells attached to the bottom of the 96-well plate. Scale bar = 500 μm. $^{**}P < .01$. (*B*) Spheroid formation assay. The solidified spheroid drops (generated from MIA-V, MIA-ZIP4, AsPC-shV, and AsPC-shZIP4 cells) were kept on the dish lid for 2, 4, and 24 hours at 37°C and then were imaged using a light microscope. Ten spheroids were included and analyzed in each group. Scale bar = 200 μm. (*C*) Matrigel-embedded organoids. The chamber slide was precoated with Matrigel at 37°C for 2 hours. Human and mouse pancreatic cancer cells were resuspended in the culture medium containing 2% Matrigel and cultured on the chamber slide for 8 days. Scale bar = 50 μm. (*D*) Matrigel-suspended organoids. Cells were resuspended in the culture medium containing 50% Matrigel in the 24-well plate for 8 days. Scale bar = 200 μm. (*E*) Hematoxylin-eosin staining of 3D organoids established from MIA-V, MIA-ZIP4, AsPC-shV, and AsPC-shZIP4 cells. Scale bar = 50 μm.

and suspended models (Figure 4*C*–*E*). Similar results were also observed in KPC and KPCZ models, in which knockout of ZEB1 decreased the size of organoids (Figure 4*C* and *D*). Integrins play an essential role on cell-to-cell and cell-to-ECM adhesion, and we found ITGA3 knockdown inhibited cell-to-ECM adhesion and spheroid formation in pancreatic cancer cells (Supplementary Figure 5*C* and *D*). Inhibition of ITGA3 also suppressed tumor growth in the xenograft tumor model (Supplementary Figure 6*A*) and increased cell-to-cell connections through upregulating F-actin level (Supplementary Figure 6*B*). Overall, these findings identify ZIP4-promoted organogenesis and cell-to-ECM adhesion via upregulation of ITGA3 in pancreatic cancer.

ZIP4 Promoted EMT in Pancreatic Cancer 3D Spheroid and Organoid Model

Having shown that ZIP4 is important for organogenesis, we sought to determine the mechanism underlying ZIP4-mediated promotion of organogenesis in pancreatic cancer using our organoid model. Integrins have a profound role on pancreatic organogenesis and tissue maintenance and promote pancreas development. Thus, we first examined the expression profile of ITGA3 in the 3D organoid model. ITGA3 signal was significantly higher in the organoid derived from cells overexpressing ZIP4 (Figure 5*A*). Similarly ITGA3 level was higher in the 3D spheroid model generated from ZIP4 overexpressing cells (Figure 5*C*). In

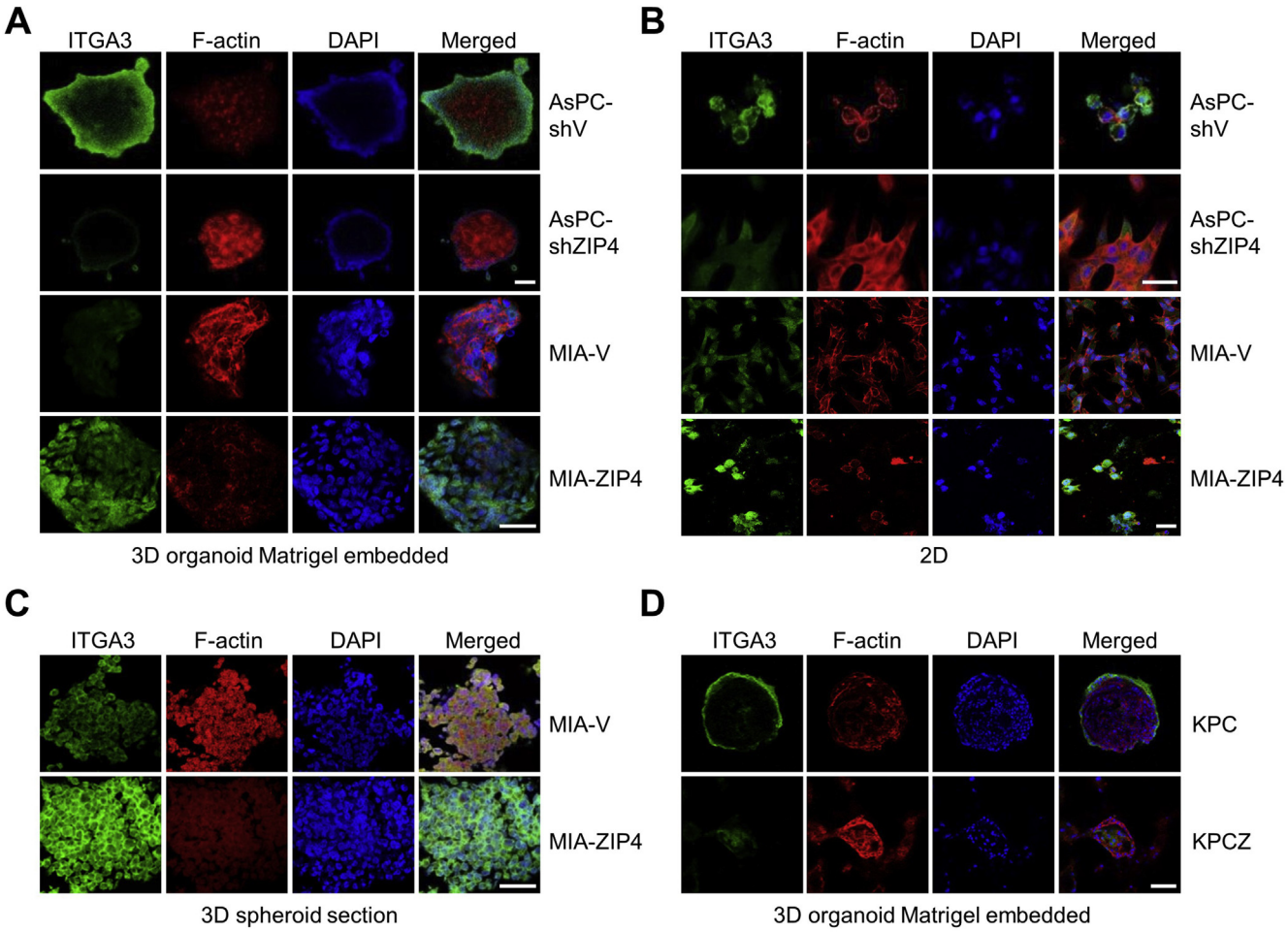

Figure 5. Expression of ITGA3 in the 3D spheroid/organoid model. (*A*) Images were taken using 3D confocal microscopy. ITGA3 was stained and F-actin was labeled in 3D organoid Matrigel-embedded model derived from AsPC-shV, AsPC-shZIP4, MIA-V, and MIA-ZIP4 cells. Scale bar = 50 μm. (*B*) Images were taken using 3D confocal microscopy. ITGA3 was stained and F-actin was labeled with 2D AsPC-shV, AsPC-shZIP4, MIA-V, and MIA-ZIP4 cells. Scale bar = 10 μm. (*C*) Images were taken using 3D confocal microscopy. ITGA3 was stained and F-actin was labeled in the 3D spheroid sectional slides. Scale bar = 50 μm. (*D*) Images were taken using 3D confocal microscopy. ITGA3 was stained and F-actin was labeled with 3D organoid Matrigel-embedded model derived from KPC and KPCZ cells. Scale bar = 50 μm.

contrast, ITGA3 signal was decreased in the organoids and spheroids derived from cell lines with ZIP4 knockdown (Figure 5*A*, 5*C*, Supplementary Figure 6*C* and *D*). We also determined the level of cytoskeletal protein F-actin in the 3D organoids and spheroids and found it to be highly expressed between cell-to-cell junctions and connection edges in the organoids and spheroids with lower levels of ZIP4 (Figure 5*A* and *C*). We also assessed the ITGA3 expression in 2D cell cultures, the differences were not as significant as that in the 3D organoid model (Figure 5*B*). We also noted that knockout of ZEB1 resulted in decreased ITGA3 in organoids derived from KPC cells, while leading to increased F-actin expression (Figure 5*D*).

Several studies indicated that EMT contributes to normal organogenesis during the development of epithelial cell.[34] In 2D culture, planar attachment inhibits cell geometry resulting in limited cell motility. In contrast, 3D systems are more appropriate for EMT studies because cancer cells acquire morphological and cellular characteristics reminiscent of in vivo tumors.[35] Thus, we assessed the morphology of spheroid sections using hematoxylin-eosin staining; when ZIP4 was overexpressed, cell-to-cell connections in the spheroid appeared less tight (Figure 6*A*) but blocking of ZIP4 increased cell-to-cell connections (Supplementary Figure 6*E*). We additionally assessed expression of EMT markers in both the 2D cell lines and the 3D spheroid model. Blocking ZIP4 in the 3D spheroid model significantly decreased vimentin and N-cadherin level but increased E-cadherin level (Figure 6*B*). When ZIP4 was overexpressed, EMT was enhanced via upregulation of vimentin and N-cadherin paired with downregulation of claudin-1 (Figure 6*C*); however, there were no significant changes in EMT marker expression in the 2D system when ZIP4 was knocked down (Figure 6*B* and *C*, Supplementary Figure 7*A* and *B*). We additionally determined levels of the ZIP4 downstream markers LATS2, YAP1, and ITGA3 in the 3D spheroid model and found significant positive correlations of YAP1 and ITGA3

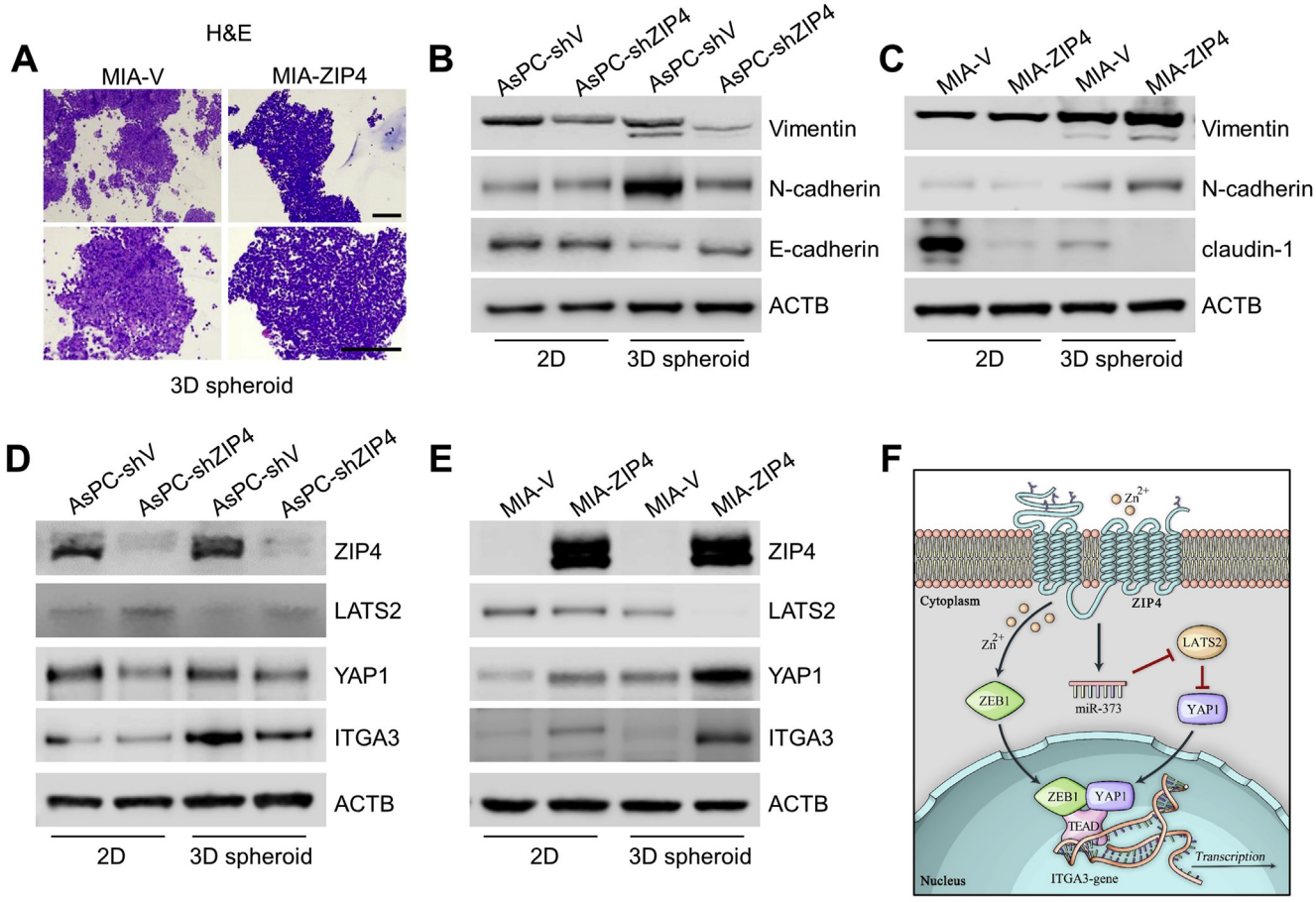

Figure 6. ZIP4 promotes EMT in pancreatic cancer. (*A*) Hematoxylin-eosin staining of 3D tumor spheroid generated from MIA-V and MIA-ZIP4 cells. Spheroids were collected after 3 days of spheroid culture and processed tissue embedding and sectioning. Scale bar = 100 μm. (*B*) Expression of EMT markers Vimentin, N-cadherin, E-cadherin, or claudin-1 was examined in AsPC-shV and AsPC-shZIP4 cells cultured under 2D and 3D conditions. (*C*) Expression of EMT markers in MIA-V and MIA-ZIP4 cells. (*D*) Protein levels of LATS2, YAP1, and ITGA3 in AsPC-shV and AsPC-shZIP4 cells cultured under 2D and 3D conditions. (*E*) Protein levels of LATS2, YAP1, and ITGA3 in MIA-V and MIA-ZIP4 cells. (*F*) Schematic diagram of the signaling axis of ZIP4-miR-373-LATS2-ZEB1/YAP1/TEAD-ITGA3.

levels with ZIP4, and reverse correlation of LATS2 level with ZIP4 (Figure 6*D* and *E*, Supplementary Figure 7*C* and *D*), and in the 3D organoid model, it is also shown that knocking down ZIP4 decreased YAP1, vimentin, and N-cadherin expression (Supplementary Figure 7*E*). Our results indicate that ZIP4 promotes EMT and organogenesis in the 3D organoid system via activation of ITGA3.

Discussion

In this study we demonstrated a novel ZIP4-miR-373-LATS2-ZEB1/YAP1-ITGA3 signaling pathway in pancreatic cancer EMT plasticity, cell-ECM adhesion, organogenesis, and metastasis (Figure 6*F*). ZEB1 and YAP1 interacted with each other to coactivate ITGA3 transcription and ZIP4 upregulated ZEB1/YAP1 and contributes to ITGA3 expression and EMT plasticity. At the same time, we found in the KPC mouse cells, knocking out ZEB1 inhibited organogenesis and apical to basal polarity.

The role of EMT in cancer metastasis is well appreciated, and EMT-induced cellular phenotype change enables cancer cells to experience dissociation, intravasation, extravasation, and macrometastasis formation.[9] EMT plasticity prompts cells to transit between EMT and MET states allowing the cells migrate from the primary tumor and colonize at the secondary tumor.[3] Nihan Kilinc et al[36] reported that transforming growth factor-β induced EMT in murine epithelial mammary carcinoma cells, but this reverted to the epithelial phenotype when transforming growth factor-β was depleted. Therefore, EMT plasticity is a dynamic transiting between EMT and MET phenotypes reversibly. Stemmler et al has recently proposed an exciting concept of partial EMT,[6,10] in which EMT program can be transient and reversible between epithelial and mesenchymal states. Partial EMT may have been activated even though no significant EMT morphologies are identified in cells. In our study, we found that there were significant differences of EMT markers between cells with ZIP4 high or low, but no morphology changes were identified between the cells. The partial EMT may help to explain this finding that EMT is still active and is not needed to experience the full EMT program. Previously we have shown ZIP4 promoted pancreatic

cancer migration and invasion through downregulation of tight junction protein ZO-1 and claudin-1, important intermediate molecules in the EMT program[32]; however, little is known about the effect of ZIP4 on EMT program in pancreatic cancer. In this study, our data indicated that ZIP4 promoted EMT plasticity in pancreatic cancer cells through a zinc-dependent regulation of EMT-TFs and coactivation. That also explained why the structure of spheroids derived from ZIP4 highly expressed cells was looser because ZIP4 promoted EMT and disrupted cell-to-cell connections in the spheroid model.

ZEB1 is a key EMT-TF in pancreatic cancer. Krebs et al[10] identified genetic depletion of ZEB1 in KC mouse model reduced ADM and PanIN-precursor lesions formation, tumorigenesis, and in the KPC mouse model, they found depletion of ZEB1 inhibited cell plasticity, invasion, and metastasis.[10] However, genetic depletion of other EMT-activators such as Snai1 or Twist1 had no effect on tumor invasion or metastasis in the KPC model.[10,37] Liu et al[38] elucidated effects of ZEB1 on tumor initiation and EMT/metastasis can be separated based on different levels of ZEB1. It is indicated that lower level of ZEB1 contributes to tumor initiation; however, further induction of ZEB1 is required for tumor metastasis, which explained why genetic depletion of Snail1 in the KPC mice had no effect on tumor invasiveness and metastasis.[10] Even though Snail1 was knocked out, ZEB1 was only partial depleted, which is not sufficient to abolish tumor metastasis. Krebs et al and Lehmann et al demonstrated that depletion of ZEB1 inhibited tumorigenic, metastasis, and cell plasticity in the KPC mouse model ZEB1.[10,12] ZEB1 is an important EMT activator in several different cancers, but less is known on how ZEB1 is activated and upregulated in pancreatic cancer. Our findings showed that as a zinc-dependent transcription factor, ZEB1 can be activated by a cancer-promoting zinc transporter ZIP4 through phosphorylation of STAT3. ZEB1 was found to directly repress miR-200 family and promoted breast cancer EMT and progress.[11] Other than transcriptional repression, ZEB1 also acts as a transcriptional activator. The dual function of ZEB1 depends on which co-transcription factor that ZEB1 interacts with. Lehmann et al[12] showed ZEB1 activated CTGF and AXL through interaction with YAP1/TEAD in breast cancer. ZEB1 can also interact with factor Lef/Tcf to activate downstream targets Nrp2 and Prex1 transcription in glioblastoma.[13] However, little is known about how ZEB1 transcriptionally activates ITGA3 in pancreatic cancer. We found in pancreatic cancer cells, among many coactivators such as Lef1, CAF, and P300, YAP1 is the only potent coactivator of ZEB1, which significantly activates ITGA3 transcription. ZEB1 usually binds to the promoter of candidate target genes through E-box known as the ZEB1 binding motif.[39] We found after the mutation of E-box binding sites at ITGA3 promoter, when ZEB1 was blocked, the promoter activity of ITGA3 was increased. Therefore, it seemed that ZEB1 did not activate ITGA3 transcription through E-box binding sites. Later we found ZEB1 interacted with YAP1/TEAD and formed a complex to coactivate ITGA3 through YAP1/TEAD binding sites at ITGA3 promoter. Our data explained how ZEB1 activates ITGA3 through its coactivator YAP1 in pancreatic cancer. ZEB1 is a zinc-dependent transcription factor and previously we have shown ZIP4 upregulates ZEB1 through phosphorylation of STAT3; however, it is unclear how ZIP4 regulates YAP1 in pancreatic cancer. Aberrant activated signaling by the Hippo pathway has been reported in lung, breast, colon, and pancreatic cancer.[40] YAP1 is the downstream effector of Hippo pathway and Meng at al[41] indicated Hippo pathway regulator LATS2 inhibits YAP1 activity through phosphorylation, cytoplasmic retention, and protein degradation. Previously we have identified LATS2 is the downstream target of miR-373, which can be downregulated by ZIP4 in pancreatic cancer.[22] Based on gene ontology analysis from TCGA pancreatic cancer database, it is shown that ZIP4 is linked to the Hippo pathway. For the first time, we demonstrated that ZIP4 is positively correlated with YAP1 in pancreatic cancer and ZIP4 upregulated YAP1 through the miR-373-LATS2 signaling axis. We further identified upregulation of ZEB1 and YAP1 through separate signaling pathways by ZIP4 contributes to ITGA3 expression in pancreatic cancer.

Cell adhesion plays a critical role in the late stage of metastasis and the secondary tumor production. It helps establish tight connections between cells to cells and cells to the matrix when the circulating cancer cells reach the distal organ sites,[4] and cell adhesion not only links cells to ECM but also activates cell proliferation and modulates tumor microenvironment to facilitate EMT plasticity and the secondary tumor formation. However, the mechanism of how ZIP4 promotes cell adhesion in pancreatic cancer was not clear. Increasing evidence shows that activated integrin signaling contributes to cell-cell adhesion, cell proliferation, and EMT. Activated $\alpha5\beta1$ integrin increased cell adhesion to fibronectin during EMT.[42] Recently Li et al summarized some clinical trials targeting integrins in cancer, and indicated integrin antagonists such as $\alpha v\beta3$ and $\alpha v\beta5$ integrins are applied more frequently in lung, liver, and prostate cancer.[43] In our study, we showed among the integrin families, integrin $\alpha3\beta1$ can be activated by ZIP4 and both high level of ZIP4 and integrin $\alpha3\beta1$ predicted poor overall survival of patients with pancreatic cancer. Also, blocking of integrin $\alpha3\beta1$ attenuated the effect of ZIP4 on pancreatic cancer progression and metastasis both in vitro and in vivo. It suggested ITGA3 may serve as a good candidate for pancreatic cancer therapy.

In summary, we have shown that ZIP4 upregulated YAP1 through the Hippo pathway and that ZIP4 promotes pancreatic cancer cell-to-ECM adhesion, organogenesis, and EMT plasticity by upregulating ITGA3, which is directly activated by ZEB1/YAP1 complex. Furthermore, we elucidated a novel signaling axis ZIP4-miR-373-LATS2-ZEB1/YAP1-ITGA3 in pancreatic cancer. Our data suggested that ZIP4 is a critical regulator of this signaling pathway and the phenotypes of EMT and tumor metastasis; thus, ZIP4

represents a novel and potentially effective therapeutic target in pancreatic cancer.

Supplementary Material

Note: To access the supplementary material accompanying this article, visit the online version of *Gastroenterology* at www.gastrojournal.org, and at https://doi.org/10.1053/j.gastro.2020.12.077.

References

1. Siegel RL, Miller KD, Jemal A. Cancer statistics, 2020. CA Cancer J Clin 2020;70:7–30.
2. Reymond N, d'Agua BB, Ridley AJ. Crossing the endothelial barrier during metastasis. Nat Rev Cancer 2013;13:858–870.
3. Chin VL, Lim CL. Epithelial-mesenchymal plasticity-engaging stemness in an interplay of phenotypes. Stem Cell Investig 2019;6:25.
4. Guan X. Cancer metastases: challenges and opportunities. Acta Pharm Sin B 2015;5:402–418.
5. Selivanova G, Ivaska J. Integrins and mutant p53 on the road to metastasis. Cell 2009;139:1220–1222.
6. Stemmler MP, Eccles RL, Brabletz S, et al. Non-redundant functions of EMT transcription factors. Nat Cell Biol 2019;21:102–112.
7. Nieto MA. The snail superfamily of zinc-finger transcription factors. Nat Rev Mol Cell Biol 2002;3:155–166.
8. Nieto MA, Huang RY, Jackson RA, et al. Emt: 2016. Cell 2016;166:21–45.
9. Yang J, Antin P, Berx G, et al. Guidelines and definitions for research on epithelial-mesenchymal transition. Nat Rev Mol Cell Biol 2020;21:341–352.
10. Krebs AM, Mitschke J, Lasierra Losada M, et al. The EMT-activator Zeb1 is a key factor for cell plasticity and promotes metastasis in pancreatic cancer. Nat Cell Biol 2017;19:518–529.
11. **Burk U, Schubert J, Wellner U**, et al. A reciprocal repression between ZEB1 and members of the miR-200 family promotes EMT and invasion in cancer cells. EMBO Rep 2008;9:582–589.
12. Lehmann W, Mossmann D, Kleemann J, et al. ZEB1 turns into a transcriptional activator by interacting with YAP1 in aggressive cancer types. Nat Commun 2016;7:10498.
13. Rosmaninho P, Mukusch S, Piscopo V, et al. Zeb1 potentiates genome-wide gene transcription with Lef1 to promote glioblastoma cell invasion. EMBO J 2018;37:e97115.
14. Kim JH, Cho EJ, Kim ST, et al. CtBP represses p300-mediated transcriptional activation by direct association with its bromodomain. Nat Struct Mol Biol 2005;12:423–428.
15. Zanconato F, Cordenonsi M, Piccolo S. YAP/TAZ at the roots of cancer. Cancer Cell 2016;29:783–803.
16. **Park J, Kim DH**, Shah SR, et al. Switch-like enhancement of epithelial-mesenchymal transition by YAP through feedback regulation of WT1 and Rho-family GTPases. Nat Commun 2019;10:2797.
17. **Nardone G, Oliver-De La Cruz J**, Vrbsky J, et al. YAP regulates cell mechanics by controlling focal adhesion assembly. Nat Commun 2017;8:15321.
18. Moroishi T, Park HW, Qin B, et al. A YAP/TAZ-induced feedback mechanism regulates Hippo pathway homeostasis. Genes Dev 2015;29:1271–1284.
19. Zhou Y, Zhang J, Li H, et al. AMOTL1 enhances YAP1 stability and promotes YAP1-driven gastric oncogenesis. Oncogene 2020;39:4375–4389.
20. Mori M, Triboulet R, Mohseni M, et al. Hippo signaling regulates microprocessor and links cell-density-dependent miRNA biogenesis to cancer. Cell 2014;156:893–906.
21. Diez-Cunado M, Wei K, Bushway PJ, et al. miRNAs that induce human cardiomyocyte proliferation converge on the Hippo pathway. Cell Rep 2018;23:2168–2174.
22. **Zhang Y, Yang J**, Cui X, et al. A novel epigenetic CREB-miR-373 axis mediates ZIP4-induced pancreatic cancer growth. EMBO Mol Med 2013;5:1322–1334.
23. Li M, Zhang Y, Liu Z, et al. Aberrant expression of zinc transporter ZIP4 (SLC39A4) significantly contributes to human pancreatic cancer pathogenesis and progression. Proc Natl Acad Sci U S A 2007;104:18636–18641.
24. Li M, Zhang Y, Bharadwaj U, et al. Down-regulation of ZIP4 by RNA interference inhibits pancreatic cancer growth and increases the survival of nude mice with pancreatic cancer xenografts. Clin Cancer Res 2009;15:5993–6001.
25. **Liu M, Zhang Y, Yang J**, et al. ZIP4 increases expression of transcription factor ZEB1 to promote integrin alpha3beta1 signaling and inhibit expression of the gemcitabine transporter ENT1 in pancreatic cancer cells. Gastroenterology 2020;158:679–692.e1.
26. **Fornes O, Castro-Mondragon JA, Khan A**, et al. JASPAR 2020: update of the open-access database of transcription factor binding profiles. Nucleic Acids Res 2020;48:D87–D92.
27. Zhao B, Ye X, Yu J, et al. TEAD mediates YAP-dependent gene induction and growth control. Genes Dev 2008;22:1962–1971.
28. Sudol M, Shields DC, Farooq A. Structures of YAP protein domains reveal promising targets for development of new cancer drugs. Semin Cell Dev Biol 2012;23:827–833.
29. **Kandasamy S, Adhikary G**, Rorke EA, et al. The YAP1 signaling inhibitors, verteporfin and CA3, suppress the mesothelioma cancer stem cell phenotype. Mol Cancer Res 2020;18:343–351.
30. Zhang Z, Du J, Wang S, et al. OTUB2 promotes cancer metastasis via Hippo-independent activation of YAP and TAZ. Mol Cell 2019;73:7–21.e7.
31. **Yang J, Zhang Z, Zhang Y**, et al. ZIP4 promotes muscle wasting and cachexia in mice with orthotopic pancreatic tumors by stimulating RAB27B-regulated release of extracellular vesicles from cancer cells. Gastroenterology 2019;156:722–734.e6.
32. Liu M, Yang J, Zhang Y, et al. ZIP4 promotes pancreatic cancer progression by repressing ZO-1 and Claudin-1

through a ZEB1-dependent transcriptional mechanism. Clin Cancer Res 2018;24:3186–3196.
33. Moreira L, Bakir B, Chatterji P, et al. Pancreas 3D organoids: current and future aspects as a research platform for personalized medicine in pancreatic cancer. Cell Mol Gastroenterol Hepatol 2018;5:289–298.
34. Campbell K. Contribution of epithelial-mesenchymal transitions to organogenesis and cancer metastasis. Curr Opin Cell Biol 2018;55:30–35.
35. Tevis KM, Colson YL, Grinstaff MW. Embedded spheroids as models of the cancer microenvironment. Adv Biosyst 2017;1:1700083.
36. Nihan Kilinc A, Sugiyama N, Reddy Kalathur RK, et al. Histone deacetylases, Mbd3/NuRD, and Tet2 hydroxylase are crucial regulators of epithelial-mesenchymal plasticity and tumor metastasis. Oncogene 2020;39:1498–1513.
37. **Zheng X, Carstens JL**, Kim J, et al. Epithelial-to-mesenchymal transition is dispensable for metastasis but induces chemoresistance in pancreatic cancer. Nature 2015;527:525–530.
38. Liu Y, Lu X, Huang L, et al. Different thresholds of ZEB1 are required for Ras-mediated tumour initiation and metastasis. Nat Commun 2014;5:5660.
39. Manshouri R, Coyaud E, Kundu ST, et al. ZEB1/NuRD complex suppresses TBC1D2b to stimulate E-cadherin internalization and promote metastasis in lung cancer. Nat Commun 2019;10:5125.
40. Wang Y, Xu X, Maglic D, et al. Comprehensive molecular characterization of the Hippo signaling pathway in cancer. Cell Rep 2018;25:1304–1317.e5.
41. Meng Z, Moroishi T, Guan KL. Mechanisms of Hippo pathway regulation. Genes Dev 2016;30:1–17.
42. Desgrosellier JS, Barnes LA, Shields DJ, et al. An integrin alpha(v)beta(3)-c-Src oncogenic unit promotes anchorage-independence and tumor progression. Nat Med 2009;15:1163–1169.
43. Li ZH, Zhou Y, Ding YX, et al. Roles of integrin in tumor development and the target inhibitors. Chin J Nat Med 2019;17:241–251.

Author names in bold designate shared co-first authorship.

Received November 2, 2020. Accepted December 29, 2020.

Correspondence
Address correspondence to: Min Li, PhD, Department of Medicine, Department of Surgery, The University of Oklahoma Health Sciences Center, 975 NE 10th Street, BRC 1262A, Oklahoma City, Oklahoma 73104. e-mail: Min-Li@ouhsc.edu; fax: (405) 271-1476.

Acknowledgments
The authors thank the Peggy and Charles Stephenson Cancer Center at the University of Oklahoma Health Sciences Center for the use of Histology and Immunohistochemistry Core, which provided RNA Basescope in situ staining, immunohistochemistry, and image analysis services. We also thank The Cancer Genome Atlas (TCGA) pancreatic cancer database. Our results shown here are in part based on data generated by the TCGA Research Network: https://www.cancer.gov/tcga.

CRediT Authorship Contributions

Mingyang Liu, PhD (Conceptualization: Lead; Data curation: Lead; Formal analysis: Lead; Investigation: Lead; Methodology: Lead; Project administration: Lead; Resources: Lead; Software: Lead; Validation: Lead; Visualization: Lead; Writing – original draft: Lead; Writing – review & editing: Lead)

Yuqing Zhang, PhD (Conceptualization: Lead; Formal analysis: Lead; Investigation: Lead; Project administration: Lead; Writing – review & editing: Lead)

Jingxuan Yang, PhD (Conceptualization: Lead; Data curation: Lead; Formal analysis: Lead; Project administration: Lead; Writing – review & editing: Lead)

Hanxiang Zhan, MD, PhD (Conceptualization: Lead; Formal analysis: Lead; Project administration: Lead; Writing – review & editing: Lead)

Zhijun Zhou, MD, PhD (Formal analysis: Lead; Software: Lead; Writing – review & editing: Lead)

Yuanyuan Jiang, MD, PhD (Formal analysis: Lead; Writing – review & editing: Lead)

Xiuhui Shi, MD, PhD (Formal analysis: Lead; Software: Lead; Writing – review & editing: Lead)

Xiao Fan, MS (Writing – review & editing: Lead). Junxia Zhang, MD (Writing – review & editing: Lead)

Wenyi Luo, MD (Methodology: Lead; Writing – review & editing: Lead)

Kar-Ming A. Fung, MD (Methodology: Lead; Writing – review & editing: Lead)

Chao Xu, PhD (Methodology: Lead; Writing – review & editing: Lead)

Michael S. Bronze, MD (Writing – review & editing: Lead)

Courtney W. Houchen, MD (Writing – review & editing: Lead)

Min Li, PhD (Conceptualization: Lead; Funding acquisition: Lead; Supervision: Lead; Validation: Lead; Visualization: Lead; Writing – review & editing: Lead).

Conflict of interest
The authors disclose no conflicts.

Funding
This work was supported in part by National Institutes of Health (NIH) grants R01 CA186338-01A1, R01 CA203108, and R01 CA247234-01; the William and Ella Owens Medical Research Foundation (Min Li), and NIH/National Cancer Institute award P30CA225520.

Supplementary Materials and Methods

Cell Viability Assay

The 96-well plate was precoated with 500 μg/mL laminin at 37°C for 2 hours. Pancreatic cancer cells were seeded onto the plate. After 30 minutes, cells were gently washed with phosphate-buffered saline 3 times and fixed with 4% paraformaldehyde (PFA) and stained with crystal violet for 1 minute. Images were taken under a light microscope. At the same time, cell viability was detected with 2 μL alamarblue (Bio-Rad, Hercules, CA) reagent mixed with 98 μL 10% fetal bovine serum medium. Absorbance was recorded at 560 and 590 nm with microplate reader (Bio-Tek Instruments, Vinooski, VT).

Western Blot Analysis

Cell lysate protein was isolated and loaded on sodium dodecyl sulfate polyacrylamide gels as previously described.[1] Membranes were incubated with appropriate antibodies against ZIP4 (Proteintech, Rosemont, IL; 1:2000), ITGA3 (Millipore, Billerica, MA; 1:1000), YAP1 (Cell Signaling Technology; 1:1000), ZEB1 (Cell Signaling Technology; 1:500), LATS2 (Cell Signaling Technology; 1:400), or β-actin (Sigma; 1:10,000) at 4°C overnight. After washing with 0.1% Tween 20–Tris-HCl-buffered saline (TBS), the membranes were incubated with a horseradish peroxidase-linked secondary antibody (1:5000) for 2 hours at room temperature. Immunoreactive bands were detected using an enhanced chemiluminescent (ECL) plus reagent kit.

Immunohistochemical Staining

Three-dimensional spheroids and xenograft tumors were collected and fixed with 4% PFA or formalin and embedded with paraffin and were sectioned into 4-μm slides. Slides were deparaffinized and incubated with 3% hydrogen peroxide solution to quench endogenous peroxidase activity for 15 minutes and then steamed for 15 minutes for the antigen retrieval and incubated in blocking buffer for 30 minutes at room temperature and incubated with antibody against YAP1 (1:500; Cell Signaling Technology), ITGA3 (1:1000; Millipore Sigma), LATS2 (1:50; Proteintech), and incubated overnight at 4°C. After washing with PBS, slides were incubated with polymer secondary antibody for 30 minutes (Vector Laboratories). Immune complexes were detected with diaminobenzidine under a phase-contrast microscope. The sections were then dehydrated, mounted, and observed under the microscope.

Immunofluorescence Staining

Human pancreatic cancer cell lines, KPC, and KPCZ mouse cells were seeded onto chamber slides and fixed with 4% PFA at room temperature for 15 minutes. The slides were treated with 0.2% Triton X-100 at room temperature for 15 minutes for the permeabilization. Slides were blocked in TBS with 0.1% bovine serum albumin for 30 minutes at room temperature and incubated with primary antibody anti-ITGA3 (1:200; Millipore Sigma), ZIP4 (1:500; Proteintech) at 4°C overnight. After washing with TBS 3 times, slides were incubated with Alexa Fluor Plus 488 secondary antibody (1:200; Thermo Fisher Scientific, Waltham, MA) at room temperature for 30 minutes. Slides were then incubated with F-actin (Abcam, Cambridge, MA) at room temperature for 1 hour, then labeled with Hoechst (1:10,000) for 1 minute. The slides were then mounted and observed under the confocal microscope.

Confocal Microscopy Imaging

Briefly, cells and spheroids were fixed with 2% PFA for 10 minutes at room temperature, permeabilized with TBS-0.2% Triton X-100 for 10 minutes and then blocked with 0.2% bovine serum albumin in TBS. Samples were incubated with primary antibodies overnight and incubated with secondary antibodies (1:200 dilution) for 1 hour at room temperature, and mounted in mounting medium (Vector Laboratories, Burlingame, CA). Confocal images were acquired using Leica (Wetzlar, Germany) SP8 with 405, 488, and 647 laser lines. Images were analyzed using LASX software (Leica).

Gene Set Enrichment Analysis

RNA-sequencing data were acquired from TCGA pancreatic cancer database (https://portal.gdc.cancer.gov/). We stratified samples into ZEB1-high and ZEB1-low groups. Gene set of YAP1 conserved signature was obtained from MSigDB database (https://www.gsea-msigdb.org/gsea/index.jsp). Gene set enrichment analysis was performed in gene set enrichment analysis software following the instructions of the software.

Supplementary Reference

1. **Kandasamy S, Adhikary G**, Rorke EA, et al. The YAP1 signaling inhibitors, verteporfin and CA3, suppress the mesothelioma cancer stem cell phenotype. Mol Cancer Res 2020;18:343–351.

Author names in bold designate shared co-first authorship.